
Genetic Reconstitution of Functional Acetylcholine Receptor Channels in Mouse Fibroblasts

TONI CLAUDIO,* W. N. GREEN, DEBORAH S. HARTMAN, DEBORAH HAYDEN, HENRY L. PAULSON, F. J. SIGWORTH, STEVEN M. SINE, ANNE SWEDLUND

Foreign genes can be stably integrated into the genome of a cell by means of DNA-mediated gene transfer techniques, and large quantities of homogenous cells that continuously express these gene products can then be isolated. Such an expression system can be used to study the functional consequences of introducing specific mutations into genes and to study the expressed protein in the absence of cellular components with which it is normally in contact. All four *Torpedo* acetylcholine receptor (AChR) subunit complementary DNA's were introduced into the genome of a mouse fibroblast cell by DNA-mediated gene transfer. A clonal cell line that stably produced high concentrations of correctly assembled cell surface AChR's and formed proper ligand-gated ion channels was isolated. With this new expression system, recombinant DNA, biochemical, pharmacological, and electrophysiological techniques were combined to study *Torpedo* AChR's in a single intact system. The physiological and pharmacological profiles of *Torpedo* AChR's expressed in mouse fibroblast cells differ in some details from those described earlier, and may provide a more accurate reflection of the properties of this receptor in its natural environment.

THE NICOTINIC ACETYLCHOLINE RECEPTOR IS THE LIGAND-gated ionic channel that binds the neurotransmitter acetylcholine (ACh) and mediates synaptic transmission between nerve and muscle. It is located in the postsynaptic membrane of the vertebrate neuromuscular junction and is composed of four different polypeptide chains with the stoichiometry $\alpha_2\beta\gamma\delta$. A particularly rich source of acetylcholine receptor (AChR) for biochemical studies is the electric organ of the marine ray *Torpedo*, and the AChR from this tissue has been the most intensively studied in terms of its structure, ligand-binding properties, and conformational transitions (1). However, the morphology of the *Torpedo* electric organ has prevented in situ cell biological and functional studies of the AChR such as biosynthesis, assembly, modulation, flux, and ligand binding. Instead, our knowledge of the functional properties of *Torpedo* AChR's has come entirely from studies on membrane fragments or on AChR's reconstituted into artificial membrane systems, and, most recently, from the transient expression of AChR's in *Xenopus laevis* oocytes with in vitro synthesized messenger RNA (mRNA) tran-

scribed from wild-type and mutated complementary DNA's (cDNA's) (2-4). This last technique has been used to great advantage in studying the functional consequences of specific mutations in the AChR cDNA's. However, studies with the oocyte expression system are limited in the types of questions that can be addressed and in the types of analyses that can be performed. Because proteins are produced only during the lifetime of the injected RNA, studies requiring that AChR's be expressed for more than a few days are not practical in this system. Also, because the cells must be individually injected, only small quantities of AChR can be produced. This latter limitation is particularly significant because a variety of standard pharmacological assays that are necessary to characterize cloned receptors and channels cannot be conducted in the oocyte system.

As an alternative, we have pursued the stable expression of *Torpedo* AChR's by introducing the four AChR subunit cDNA's into the genomes of cultured cell lines. With this system, large numbers of identical cells are readily obtained that are amenable to biochemical, cell biological, pharmacological, and physiological characterization. We now report here the first stable expression of a protein of this complexity, obtained by cotransfecting the four AChR subunit cDNA's and a selectable marker gene into mouse fibroblast cells. We show that the subunits were assembled into complexes of the proper size and inserted into the plasma membrane where they are fully functional. Ligand-binding studies and electrophysiological recordings from *Torpedo* AChR's in the same intact cells are presented. The pharmacological and physiological data collected thus far suggest that our stable expression system may more closely parallel the native *Torpedo* membrane environment than other systems used to characterize *Torpedo* AChR's. We also found, quite unexpectedly, that expression of functional *Torpedo* AChR's in mouse fibroblasts was strongly temperature sensitive.

Expression system. Although DNA-mediated gene transfer by the calcium phosphate precipitation method is inefficient for the stable introduction of material into the genome of cells (about one transfectant in 10^3 to 10^5 cells), cells that have integrated a selectable marker gene can be readily identified, and co-introducing a gene or cDNA with that selectable marker can be very effective (5). In order to express a multisubunit protein such as the AChR, four different

T. Claudio, W. N. Green, D. Hayden, F. J. Sigworth, S. M. Sine, and A. Swedlund are in the Department of Cellular and Molecular Physiology, Yale University School of Medicine, 333 Cedar Street, New Haven, CT 06510. D. S. Hartman is in the Department of Biology, Yale University, 219 Prospect Street, New Haven, CT 06511. H. V. Paulson is in the Department of Cell Biology, Yale University School of Medicine, 333 Cedar Street, New Haven, CT 06510.

*To whom correspondence should be addressed.

cDNA's must be introduced into the same cell. We recently showed that 80 percent of fibroblast cells that integrated a selectable marker gene also integrated copies of the four subunit cDNA's (4). In our study, we have engineered the four *Torpedo* AChR cDNA's (4, 6) into a simian virus 40 (SV40) expression vector. Murine fibroblast L cells deficient in thymidine kinase (tk^-) and adenine phosphoribosyltransferase (Ltk^-aprt^-) were transfected with these DNA's plus a *tk* gene (7) by calcium phosphate precipitation (8, 9). The tk^+ transformants were put into selective medium, and 11 colonies were isolated with the use of cloning cylinders, and grown into stable cell lines. One of these cell lines, "all-11," is described below.

Characterization of integrated DNA. DNA from the all-11 cell line was subjected to Southern blot analysis (10, 11) in order to determine the integrity and the copy number of each of the integrated cDNA's. By comparing the sizes of the cDNA's integrated into the genome with the starting plasmid DNA's (Fig. 1), it appeared that the majority of the subunit cDNA's were integrated intact. A comparison of the intensities of the α , β , γ , and δ bands with that of an integrated single copy cDNA [an α cDNA introduced into NIH 3T3 cells with a retrovirus recombinant and viral infection (12)] indicated that the copy number for each of the

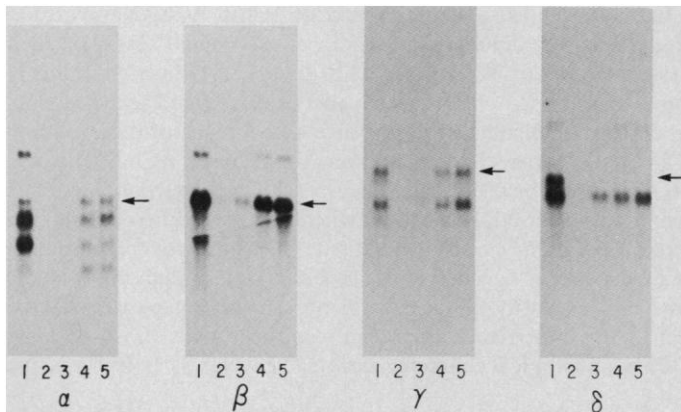


Fig. 1. DNA blots of the all-11 cell line. Genomic DNA's probed with α , β , γ , and δ sequences are marked α , β , γ , and δ ; the plasmid preparations digested with the same restriction enzymes as the genomic DNA are preceded by "p." The transfecting DNA's were prepared as follows. The dihydrofolate reductase gene was removed from the vector pSV2-DHFR (40) with a Hind III-Bgl II digestion, and a single Bgl II cloning site was created with Bgl II linkers (1001, New England Biolabs). The full-length α and β clones were isolated from our *Torpedo californica* electric organ λ gt10 cDNA library (4) with Eco RI digestions, the 1625-base pair (bp) Nco I to Pvu II fragment from the γ clone (6) and the ~1770-bp Sac I to 3' Eco RI linker fragment from our δ clone (4) were also isolated. The ends of all of these inserts were filled in with the Klenow fragment of DNA polymerase I, and Bcl I linkers (1009, New England Biolabs) were phosphorylated with polynucleotide kinase and ligated to the termini. Each of these cDNA's was inserted into the Bgl II cloning site of pSV2. Ltk^-aprt^- cells were transfected with these DNA's by the calcium phosphate precipitation procedure of Graham and van der Eb (8) as modified by Wigler *et al.* (9). The plasmid (7) ptk (50 μ g) and 5 μ g each of pSV2- α , pSV2- β , pSV2- γ , and pSV2- δ were introduced into 5×10^5 Ltk^-aprt^- cells on 10-cm plates (4). tk^+ transformants were selected in Dulbecco's modified Eagle's medium (DMEM) containing 10 percent calf serum and hypoxanthine at 15 μ g/ml, aminopterin at 1 μ g/ml, and thymidine at 5 μ g/ml ($1 \times$ HAT). Genomic DNA was prepared from a confluent 10-cm dish of cells (41). DNA that would be probed for α , β , and δ sequences was digested with Sty I (New England Biolabs). DNA to be probed for γ sequences was digested with Pvu II and Eco RI. Digested DNA (5 μ g) was loaded onto 1 percent agarose gels and blotted (11). Probes for each of the cDNA's were as follows. A 1090-bp Pvu II-Pst I fragment for α ; a 700-bp Bgl II fragment for β ; a 1290-bp Bgl II-Eco RI fragment for γ , and a 450-bp Hind III fragment for δ . Each was radiolabeled with (^{32}P) by means of the multiprime labeling system (Amersham) (42) and had specific activities of $\sim 10^7$ cpm per microgram of DNA.

cDNA's was approximately 4:2:2:8 for α , β , γ , and δ , respectively. The observations that most of these DNA's were correctly integrated and that the copy numbers varied somewhat, are consistent with our earlier report (4) in which the integrated cDNA's from 11 cell lines were analyzed after cotransfection of the four *Torpedo* AChR subunit cDNA's and *aprt*.

RNA was isolated from the all-11 cell line and subjected to Northern blot analysis to determine whether transcripts were being made, the sizes of the transcripts, and the relative levels of each. For each subunit, a transcript of the proper size was observed (arrows in Fig. 2). The amount of the different subunit RNA transcripts varied but were consistent with the number of integrated copies of each cDNA (Fig. 1). The explanation of the multiplicity of transcripts has not yet been determined. Because polyadenylation signals (13) in the 3' untranslated regions of the cDNA's were not removed, the smaller transcripts could be explained if these sites were used for polyadenylation instead of the site provided in the SV40 vector. It is also possible that the smaller RNA's seen in the α and γ blots were transcribed from incorrectly integrated cDNA's (see Fig. 1). A third possibility is that the smaller transcripts seen in the γ and δ blots were due to aberrant splicing (14).

As discussed below, we found that the presence of sodium butyrate (15) in the medium and incubation of the cells at temperatures lower than 37°C were both critical for expression of *Torpedo* AChR's in cultured cells. We therefore examined the effects of sodium butyrate and temperature on transcription. The presence of 10 mM sodium butyrate for 2 days greatly increased the transcription (Fig. 2, lanes 1 and 2). The temperature effect on some of the transcripts was also noteworthy; for example, a different sized transcript was seen in the δ blot at 37°C (Fig. 1, lane 1) compared with 28°C (lanes 3 to 5).

Expression of toxin binding sites and proper subunit polypeptides. To test for expression of cell surface AChR complexes, we incubated cells with ^{125}I -labeled α -bungarotoxin (BuTx) for 90 minutes, removed the unbound toxin, and counted the cells in a gamma counter. We were unable to detect any toxin binding activity unless all-11 cells were grown in the presence of sodium butyrate and at a reduced temperature (Fig. 3A). The optimum temperature was not determined; but at 28°C, the maximum expression of [^{125}I]BuTx-binding sites expressed on the cell surface was ~ 52 fmol per 35-mm dish ($\sim 12,600$ AChR's per cell). The internal pool of BuTx-binding AChR's was small, about 10 percent of the number of surface AChR's. At 28°C, expression reached a peak between days 5 and 7 (Fig. 3A). The decline of AChR expression after cells were cultured for 7 days in sodium butyrate at 28°C was due to cell death caused, in part, by the toxic effects of sodium butyrate on cell viability. Thus, although the cDNA's were stably integrated into the genome of cells and the subunits were expressed constitutively at low levels, transcription was greatly enhanced by the presence of sodium butyrate and expression of functional AChR's was temperature-sensitive, enabling us to regulate AChR expression.

To analyze the expressed proteins, we incubated a confluent 10-cm dish of cells with sodium butyrate for 2 days at 37°C or for 5 days at 28°C. The cells were then metabolically labeled with [3H]leucine, solubilized, and immunoprecipitated (12) with a mixture of antisera to *Torpedo* α , β , γ , and δ (anti- α , - β , - γ , and - δ) (16). The labeling pattern was identical for the two incubation conditions and all four of the subunit polypeptides were observed (Fig. 3B). The migration of each of the subunits was the same as that of native AChR subunits isolated from *Torpedo californica* electroplaque tissue, except for the γ subunit. With this subunit, the polypeptide synthesized in mouse fibroblasts appeared to migrate as if it were ~ 3000 daltons smaller than when synthesized in electroplaque. The altered migration may be due to differences in glycosylation between

mouse and *Torpedo* cells rather than to some difficulty with the γ clone, since all of the clones encode proper AChR subunits (4, 12). Because the γ subunit contains the greatest number of asparagine-linked glycosylation sites [four to five (6) compared with one each for α and β , and three for δ (17)], one would expect this subunit to be most affected by being processed in a foreign environment (18).

In addition to the four AChR subunit bands, four other bands were observed (Fig. 3B)—at ~80 kD, 28 kD, 26 kD, and 20 kD. When dishes of labeled cells were immunoprecipitated separately, with antisera to α , β , γ , and δ subunits, the band at ~80 kD was seen in all lanes indicating that it was precipitated nonspecifically. The band at ~28 kD was recognized only by anti- α and the bands at ~26 kD and ~20 kD were recognized by anti- γ . The subunits were not all produced at the same level but the level of expression was, for the most part, consistent with the level of transcription (Fig. 2) and with the number of integrated cDNA's (Fig. 1).

Subunit composition and stoichiometry. Although our all-11 cell line expressed each of the four AChR subunits, and molecules were capable of binding BuTx, the question remained whether the

Fig. 2. RNA blots of all-11 cells showing temperature and sodium butyrate effects on transcription. The arrows indicate the transcripts that were polyadenylated with the use of signals provided in the SV40 vector. When a 10-cm dish of cells was just confluent (~10⁷ cells), the medium was replaced with DMEM containing 10 percent calf serum, 1× HAT, and 10 mM sodium butyrate (SB medium), and the cells were either grown for 2 days at 37°C and 5 percent CO₂ (lane 1) or moved to an incubator maintained at 28°C and 5 percent CO₂ (lanes 2 to 5). Cells were harvested after 0 (lane 2), 2 (lane 3), 5 (lane 4), or 6 (lane 5) days at 28°C. RNA was prepared according to Chirgwin *et al.* (43). RNA (10 μ g) was subjected to electrophoresis on 1% agarose gels and blotted according to standard procedures (10) with the use of the same subunit-specific cDNA probes described in the legend to Fig. 1.

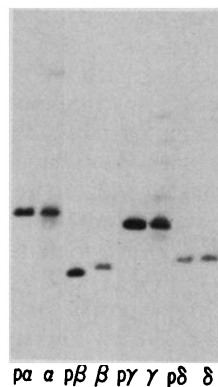
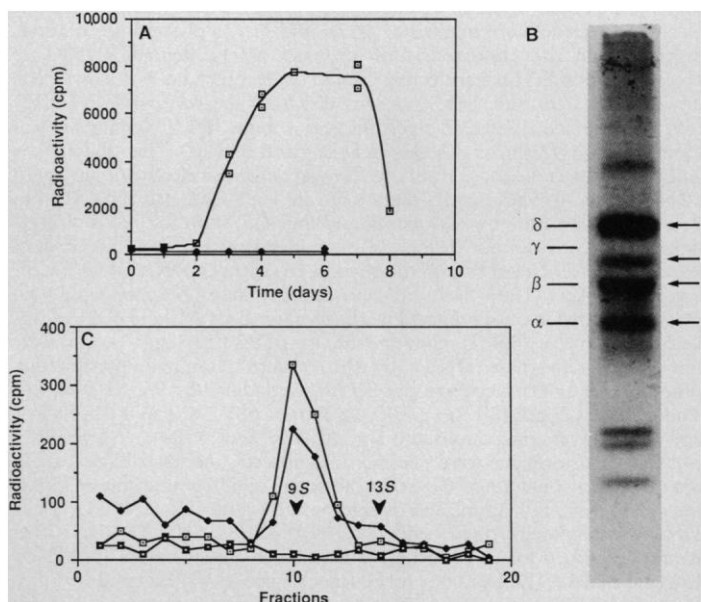


Fig. 3. Expression of *Torpedo* AChR's in mouse fibroblast cells. (A) Time course of surface AChR expression in all-11 cells. All-11 cells were grown in 35-mm dishes at 37°C in DMEM, 10 percent calf serum, and 1× HAT until just confluent. Sodium butyrate (10 mM) was added, and the cells were either kept at 37°C (filled squares) or were moved to an incubator maintained at 28°C (open squares) for 0 to 8 days. Dishes were labeled in 740 μ l of phosphate-buffered saline (PBS) containing 0.03 percent bovine serum albumin (BSA) and 0.35 nM [¹²⁵I]BuTx (1000 cpm/fmol) for 90 minutes, washed three times in 5 ml in PBS-BSA, solubilized in 1.0 ml of 1.0 percent Triton X-100, and counted in a gamma counter (B) Subunit expression in all-11 cells. The positions of AChR subunits isolated from *Torpedo californica* electroplaque tissue are marked α , β , γ , and δ . Arrows indicate the positions of *Torpedo* subunits isolated from all-11 cells. A 10-cm dish of cells was grown for 2 days at 37°C in SB medium (see legend to Fig. 2). The cells were incubated in leucine-depleted medium for 15 minutes and then 400 μ Ci of [³H]leucine (Amersham) was added, and labeling continued for 20 minutes. The cells were next harvested, solubilized in a buffer containing 1 percent Triton X-100, incubated with a mixture of antisera to *Torpedo* α , β , γ , and δ , followed by Protein A-Sepharose (Sigma) (12). Immunoprecipitates were analyzed on 10 percent SDS-polyacrylamide gels and treated for fluorography. (C) Sedimentation coefficient of *Torpedo* AChR's expressed in mouse fibroblasts. The filled diamonds indicate the profile of all-11 cells labeled with [¹²⁵I]BuTx in the presence of 10 mM dithiothreitol; the open squares indicate the profile of all-11 cells labeled with [¹²⁵I]BuTx in the absence of dithiothreitol; the filled squares indicate the profile of all-11 cells that were first incubated with 20 mM carb and then labeled with [¹²⁵I]BuTx in the continued presence of carb; the arrows mark the position of the 9S monomeric and 13S dimeric AChR complexes isolated from *Torpedo* electroplaque tissue (determined by running a parallel gradient of *Torpedo* electroplaque AChR's labeled with [¹²⁵I]BuTx). A 10-cm dish of

receptor subunits had associated into proper $\alpha_2\beta\gamma\delta$ complexes. Fujita *et al.* (19) presented evidence that, in yeast, transiently expressed *Torpedo* α subunits were inserted into the plasma membrane in the absence of the other subunits and bound BuTx with low affinity ($K_D \sim 10^{-5}M$). However, we found that when a single α subunit cDNA was stably expressed in mammalian cultured cell lines (either fibroblast or muscle cells), α subunits were not inserted into the plasma membrane although these internally expressed α subunits were capable of low-affinity BuTx binding (12). Because our assays were performed with nanomolar concentrations of toxin such that low affinity toxin binding would not be detected, and because α subunits are not expressed on the surface of this system, our results suggested that the BuTx binding we were observing on the surface of all-11 cells was not due to toxin binding to isolated α subunits. That AChR complexes were indeed formed was demonstrated directly by measuring the sedimentation coefficient of the BuTx-binding material. If the subunits had associated into proper $\alpha_2\beta\gamma\delta$ pentamers, then the molecules should migrate on sucrose gradients with a sedimentation coefficient of 9S (~250 kD) (1). A plate of all-11 cells was surface labeled with [¹²⁵I]BuTx, solubilized in a buffer containing 1 percent Triton X-100, and layered onto 5 to 20 percent sucrose gradients. The [¹²⁵I]BuTx-binding material migrated at 9S (Fig. 3C), and comigrated precisely with the 9S "monomeric" peak of AChR produced in electroplaque.

In *Torpedo*, unlike any other source of AChR, AChR's also exist as disulfide linked "dimers" that migrate at 13S (~500 kD) (1). When treated with reducing agents, AChR dimers are converted to the 9S form. We harvested AChR's from all-11 cell lines and analyzed them on sucrose gradients in the presence and absence of dithiothreitol (Fig. 3C). Under either condition, the *Torpedo* AChR's isolated from mouse fibroblast cells always migrated as monomeric 9S complexes. We do not know whether some other component present in *Torpedo* electroplaque tissue is required for the formation of AChR dimers or whether the lack of dimers is due simply to the low surface density of AChR's in our system compared with the density in electroplaque (~15/ μ m² compared with 10⁴/ μ m²).

Pharmacological characterization. We were able to harvest large



confluent all-11 cells was grown for 5 days at 28°C in SB medium. Cells were incubated for 90 minutes with [¹²⁵I]BuTx, harvested in a Triton X-100 containing buffer, centrifuged on 13-ml sucrose gradients (5 to 20 percent), and 0.6-ml fractions were collected. Portions (50 μ l) of each fraction were counted in a gamma counter, and the profiles are shown in (C).

quantities of the all-11 clonal cell line to examine the pharmacological properties of *Torpedo* AChR's expressed in intact cells. The overall pharmacological profile was qualitatively similar to that determined for AChR's in membrane fragments of *Torpedo* electroplaque and for AChR's in intact cells from the mouse muscle cell line, BC₃H-1 (20). The agonist binding properties were, however, quantitatively different from those of *Torpedo* membranes, but closely matched those of intact BC₃H-1 cells.

The kinetics of [¹²⁵I]BuTx binding to intact all-11 cells were examined (Fig. 4, A and B). The time course of association revealed that BuTx bound with high specificity with a forward rate constant of $2.2 \pm 0.3 \times 10^5 M^{-1} sec^{-1}$ ($\pm SE$). This rate constant was close to that estimated for BuTx binding to *Torpedo* AChR membranes (21) and for α -neurotoxin binding to AChR's of intact BC₃H-1 cells (20). Toxin dissociated very slowly (Fig. 4B), with a rate constant of $1.75 \pm 0.13 \times 10^{-5} sec^{-1}$ ($\pm SE$). This dissociation rate was comparable to that for intact BC₃H-1 cells (22), but was about twice that for *Torpedo* AChR membranes (23). The ratio of dissociation to association rate constants gave a dissociation constant of $7.8 \times 10^{-11} M$.

Receptor occupancy by unlabeled agonists and antagonists was examined by their competition against the initial rate of [¹²⁵I]BuTx binding (21). The competition against toxin binding for the classical antagonist, dimethyl-*d*-tubocurarine (DMT) is shown in Fig. 4C. Fitted by the empirical Hill equation (24), the competition curve is described by a dissociation constant of $2.5 \mu M$ and a Hill coefficient of 0.69. The less-than-unity Hill coefficient is consistent with measurements from BC₃H-1 cells (20, 25) and *Torpedo* membrane fragments (26) which show that reversible antagonists exhibit different affinities for the two binding sites on the receptor. Analyzed according to the two-site model (25), the competition data reveal dissociation constants of $0.52 \mu M$ and $12.0 \mu M$. This asymmetry seen in dissociation constants is similar to the asymmetry seen for BC₃H-1 ($0.3 \mu M$ and $28 \mu M$ (25) and *Torpedo* ($0.5 \mu M$

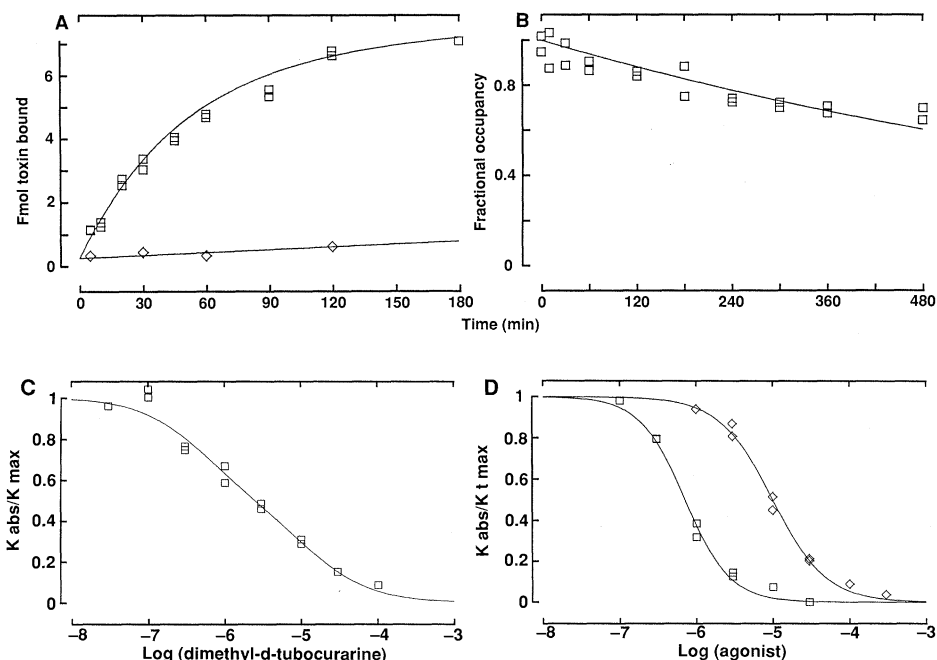
and $10 \mu M$) (26) AChR's.

Toxin is displaced in the presence of the agonists ACh and carbamylcholine (carb) (Fig. 4D). The competition curves are described by dissociation constants $K_D = 0.71$ and $10 \mu M$ and Hill coefficients $n_H = 1.48$ and 1.25 for ACh and carb, respectively. The relative affinities of these agonists are similar to those determined for AChR's from *Torpedo* membranes. The absolute dissociation constants are however 20 to 30 times greater and the Hill coefficients are larger than those measured (27) in *Torpedo* membranes [$K_D = 0.024$ (ACh) and $0.5 \mu M$ (carb); $n_H = 1.1$ (carb)]. The difference in binding parameters can be accounted for (28) by a larger allosteric constant in the *Torpedo* membrane preparation, representing a shift of the allosteric equilibrium toward the high-affinity, desensitized state of the AChR. That this shift may be due to membrane disruption is suggested by the difference in binding of carb in intact BC₃H-1 cells ($K_D = 11 \mu M$, $n_H = 1.5$) and in membrane fragments from these cells [$K_D = 1 \mu M$, $n_H = 1.0$ (29)]. Thus, it may be that our expression system allows us to measure ligand-binding properties of the *Torpedo* AChR that more closely reflect those of its native environment.

Functional characterization. Initially, a ²²Na flux assay was used to demonstrate that cell surface AChR complexes facilitated ion flux into cells in response to agonist. ACh at $60 \mu M$ induced a rapid uptake of ²²Na, and this uptake was reduced to identical background levels by prior incubation with $100 nM$ BuTx, $100 \mu M$ DMT, or prior exposure to $60 \mu M$ ACh (Fig. 5A). ACh-induced tracer uptake thus demonstrated expected pharmacological properties of AChR's, such as susceptibility to block by BuTx and DMT, and ACh-induced desensitization.

Whole-cell current recordings (30) also showed an ACh-activated response. The response of an all-11 cell to a "puff" of $30 \mu M$ ACh is shown in Fig. 5B. At a membrane potential of $-40 mV$, application of ACh elicited a rapid inward current of $\sim 50 pA$ which, in the continued presence of ACh desensitized with a time constant of 3.5

Fig. 4. Pharmacological properties of the *Torpedo* AChR's in all-11 cells. **(A)** Time course of α -bungarotoxin association. After the growth medium was aspirated, all-11 cells were covered with normal mammalian saline ($140 mM$ NaCl, $2.5 mM$ KCl, $10 mM$ Hepes, $1.8 mM$ MgCl₂, pH 7.4) containing [¹²⁵I]BuTx ($1.62 nM$), and bound toxin was measured at the specified times. The squares represent binding measured in the presence of toxin alone, while the diamonds show nonspecific binding measured with toxin in the presence of $10 mM$ carb. A least-squares fit of the specific binding component yielded a maximum binding of $6.4 fmol$ and an association rate of $2.25 \times 10^5 M^{-1} sec^{-1}$. **(B)** Time course of BuTx dissociation. The fractional occupancy is plotted as the ratio of specific toxin-receptor complexes at the indicated time to the specific complexes immediately after removal of unbound toxin. The curve represents the least-squares fit to fractional occupancy = $\exp(-k_{diss}t)$ where the fitted dissociation rate constant k_{diss} is $1.75 \times 10^{-5} sec^{-1}$. **(C)** Competition between DMT and BuTx. Cells were exposed to the specified concentrations of DMT for 30 minutes, and then the initial rates of toxin binding were measured for 30 minutes. The curve is the least squares fit to the two-site model (25) with the following parameters: $K_A = 0.52 \mu M$, $K_B = 12.0 \mu M$. In this experiment the total number of toxin sites was $15.1 fmol$ per 35-mm dish. **(D)** Competition between agonists and BuTx. Cells were incubated with the specified concentrations of either ACh (diamonds) or carb (squares) for 30 minutes, and then the initial rates of toxin binding were measured by incubation with toxin ($0.98 nM$) for 30 minutes; k_{obs} is the toxin association rate constant in the presence of ligand,



and k_t is the rate constant in the absence of ligand. The rate constants were calculated as described (20). The curves represent least-squares fits to the Hill equation with the following fitted parameters: for ACh, $K_D = 0.71 \mu M$ and $n_H = 1.48$; for carb, $K_D = 9.95 \mu M$ and $n_H = 1.25$. The total number of toxin sites was $15.1 fmol$ per 35-mm dish.

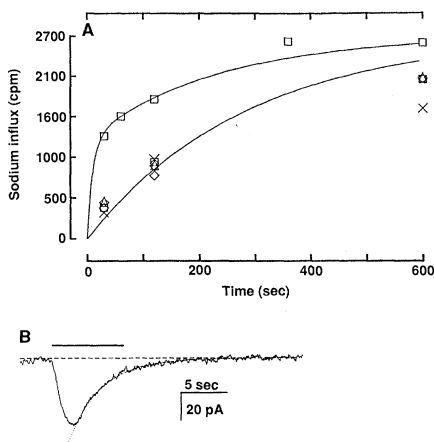
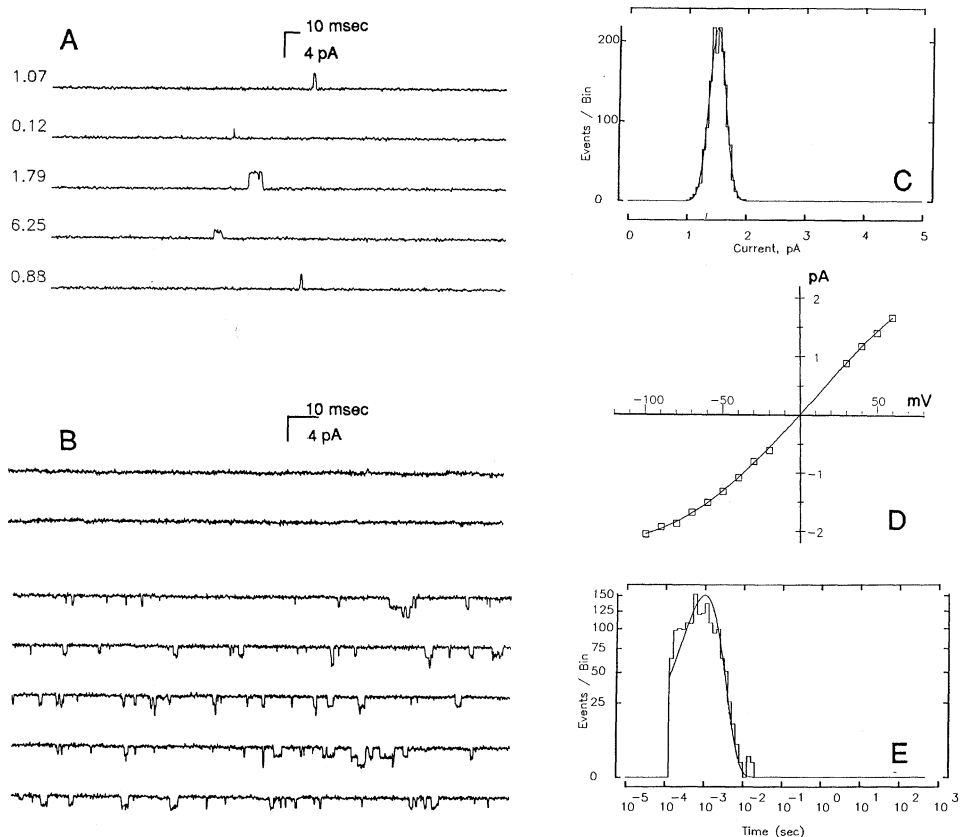


Fig. 5. Functional studies. (A) Time course of ACh-induced tracer sodium uptake by all-11 cells. Squares represent ^{22}Na uptake after the instantaneous addition of $60\ \mu\text{M}$ ACh in normal mammalian saline; diamonds are the uptake after 30 minutes of prior exposure to $60\ \mu\text{M}$ ACh; crosses are the uptake measured following the instantaneous addition of $60\ \mu\text{M}$ ACh, but with cells treated with $100\ \text{nM}$ BuTx for 30 minutes; triangles are

uptake measured in the presence of $100\ \mu\text{M}$ DMT and $60\ \mu\text{M}$ ACh; and the lower squares are the uptake measured in the absence of ACh. The curve through the squares (instantaneous ACh addition) is the visual fit to: $\text{cpm}(t) = A_0 \{1 - \exp[-k_g(t)]\}$, where $k_g(t) = k_0/k_D [1 - \exp(-k_D t)] + k_F t$ (44); k_0 is the permeability shut-off by desensitization; k_F is the permeability resistant to desensitization; and k_D is the rate constant of desensitization onset. The fitted parameters are $k_0 = 0.054\ \text{sec}^{-1}$, $k_F = 0.0042\ \text{sec}^{-1}$, and $k_D = 0.081\ \text{sec}^{-1}$. The lower curve is fitted with the following parameters: $k_0 = 0$, $k_F = 0.0035\ \text{sec}^{-1}$, and $k_D = 0$. In this experiment, the total number of toxin sites was $8.4\ \text{fmol}$ per 35-mm dish of cells. (B) Current response of an all-11 cell to the application of ACh, which was applied (at $30\ \mu\text{M}$) by pressure ejection from a $1\text{-}\mu\text{m}$ pipette for 7 seconds (indicated by the horizontal bar). The downward deflection of the current trace during the ACh puff indicates an increased inward current from the holding current level of $-14\ \text{pA}$ (dashed line). The dotted curve shows the fit of a single exponential to the decay of the current with a time constant of 3.5 seconds. All-11 cells were grown in 35-mm dishes at 28°C for 7 days in SB medium. Before recording, the medium was replaced with normal mammalian saline plus $1\ \mu\text{M}$ atropine. The pipette solution was $142\ \text{mM}$ CsCl, $5\ \text{mM}$ NaCl, $2\ \text{mM}$ MgCl_2 , $1\ \text{mM}$ EGTA, $10\ \text{mM}$ Hepes, pH 7.4. The trace was recorded in the whole cell configuration (30) at room temperature, the cell membrane capacitance was $44\ \text{pF}$.

Fig. 6. Single channel recordings from all-11 cells. (A) Cell-attached recording with the pipette held at $+50\ \text{mV}$ and containing a Cs^+ , Mg^{2+} solution (in mM : $150\ \text{CsCl}$, $5.4\ \text{KCl}$, $2\ \text{MgCl}_2$, $1\ \text{EGTA}$, $10\ \text{Hepes}$; pH 7.4) at 15.5°C . Inward currents are plotted upward and numbers to the left indicate the silent intervals (in seconds) between events. In this recording about 10 percent of the events had a low amplitude (as in the fourth trace). (B) Recordings from an outside-out patch at $-60\ \text{mV}$ and 15.5°C . The first two traces were obtained immediately after ACh was added to the bathing solution. The last five traces are from the same recording 5 seconds later, after ACh has diffused from the point of application to the membrane. ACh was added to a final bath concentration of $2\ \mu\text{M}$ in normal mammalian saline; the pipette solution (in contact with the inside of the membrane) was the same Cs^+ solution as in (A). (C) Step amplitude histogram obtained from events longer than $0.5\ \text{msec}$ in a later part of the recording shown in (B) at $-60\ \text{mV}$. The amplitudes cluster into a single peak at $-1.50 \pm 0.1\ \text{pA}$ (SD) and no low-amplitude events were observed in this outside-out patch. (D) Single channel current-voltage (i - V) relation. Points were obtained from fits to distributions as in (C); the curve is a quartic polynomial fit. The slope conductance at $0\ \text{mV}$ was $29\ \text{pS}$. (E) Open-time distribution from the outside-out patch at $-60\ \text{mV}$. The smooth curve is a fitted single-exponential distribution (time constant $1.0\ \text{msec}$) transformed to correspond to the logarithmically binned histogram (45).



seconds. This desensitization rate is similar to the slow desensitization rate observed for AChR's in both native and reconstituted membranes (31). A fast desensitization process (time constant $\sim 100\ \text{msec}$) has also been detected (31). However, because our agonist application was not sufficiently fast and uniform, we would not expect to resolve the onset of fast desensitization.

Single channel recordings from all-11 cells showed ACh-induced current pulses having the properties expected for single *Torpedo* AChR currents. In cell-attached recordings obtained with $2\ \mu\text{M}$ ACh in the recording pipette, pulses of inward current lasting $\sim 1\ \text{msec}$ and having the amplitude expected for AChR channels were observed (Fig. 6A). To verify that these events arose from ACh-activated channels, we used outside-out patch recordings (30) in which currents could be recorded before and during the application of ACh. In a patch obtained from cells showing $19\ \text{fmol}$ of BuTx sites per 35-mm culture dish, a flat baseline level of current was observed before and immediately after ACh was added to the bath solution (Fig. 6B), but a high level of channel activity appeared as ACh reached the membrane patch (Fig. 6B). A stretch of this recording 5 minutes later (after desensitization had decreased the frequency of channel openings and thus the probability of overlapping events) was used for quantitative analysis. Amplitude histograms (Fig. 6C) showed a single class of events, whose current-voltage curve (Fig. 6D) gave a slope conductance of $29\ \text{pS}$ at 15°C . This level of conductance, and the saturation of current at large negative potentials, are consistent with measurements on *Torpedo* AChR's in oocytes when the lower permeability of Na^+ and block by Mg^{2+} are taken into account (29, 32). The conductance also lies within the range of reported values in reconstituted systems [$28\ \text{pS}$ (33) and $41\ \text{pS}$ (34); both obtained with Na^+ and at room temperature]. Cell-attached recordings in which Cs^+ carried the inward current showed larger single-channel currents (Fig. 6A), as would be expected from the selectivity of the *Torpedo* AChR.

The record was also analyzed to estimate the mean channel open

duration. The distribution of open durations is reasonably described by a single exponential (Fig. 6E) with a time constant of 1 msec. Since only one in ten openings showed brief duration closures, the mean open time is essentially the same as the mean burst duration, and it corresponds closely to that measured for *Torpedo* receptors expressed in *Xenopus* oocytes. A small excess of brief duration openings is also seen (not fitted); brief openings have been observed for most AChR's from skeletal muscle. In sum, the single-channel properties of the *Torpedo* AChR expressed in all-11 cells appear to be the same as those of this same AChR expressed in *Xenopus* oocytes.

Prospects. If a fully functional nicotinic AChR is to be expressed, four different subunits must be correctly processed and assembled into an $\alpha_2\beta\gamma\delta$ pentameric complex. Although DNA mediated gene transfer is an inherently inefficient process, we have shown that the simultaneous introduction of all four cDNA's along with a selectable marker gene into the genome of mouse fibroblast cells can be achieved with high efficiency (4). Even though different copy numbers of each cDNA were introduced into the all-11 cell line and different levels of transcription and protein expression were observed, AChR subunits were assembled into proper complexes, and the complexes were inserted into the plasma membrane where they were fully functional. Thus, this method of gene transfer appears to be suitable for introducing genes or cDNA's of proteins into cells that are composed of multiple subunits.

The *Torpedo* AChR's expressed in fibroblasts have the same general characteristics as *Torpedo* AChR's studied in other systems. Our electrical recordings on all-11 cells show ACh-activated channels having desensitization kinetics, single-channel conductance, and lifetimes similar to those already seen in the transient expression of *Torpedo* AChR's in *Xenopus* oocytes. In addition, our stable expression system has allowed us to perform ligand-binding and competition experiments that until now have only been possible with membrane fragment preparations. Like the results from those preparations, we observe the same rank order of affinity of agonists and antagonists, find that antagonists exhibit different affinities for the two ACh binding sites, and observe high-affinity binding of BuTx ($K_D = 7.8 \times 10^{-11}M$).

One difference that we have observed in toxin-displacement experiments is that the equilibrium binding of ACh and carb have larger dissociation constants and Hill coefficients than have been reported in *Torpedo* membrane fragments. When interpreted in terms of an allosteric model for desensitization of the AChR, the weaker binding in the all-11 cells represents a shift of the allosteric equilibrium away from the desensitized state. Whereas in membrane fragment preparations 10 to 30 percent of the AChR's are in the desensitized state in the absence of agonist (27, 31), our binding parameters, which are very close to those obtained for AChR's in the mammalian cell line BC₃H-1, would predict that only $\sim 10^{-4}$ of the receptors are desensitized in the absence of agonist. It could be argued that the foreign membrane environment of the all-11 cells shifts the allosteric equilibrium away from the naturally high level of desensitization in a *Torpedo* AChR to a level similar to that of mammalian AChR's. However, we favor the opposite conclusion, that the all-11 cell line is providing us the first view of the *Torpedo* AChR's true ligand-binding properties in an intact membrane. In membrane fragments, the observed high level of resting desensitization could likely have arisen through the procedure of membrane disruption, as appeared to be the case in a study with BC₃H-1 membrane fragments (29). Whatever the interpretation of the weaker agonist binding that we observe, the ability to measure the binding is in itself an example of the advantage of the stable expression system, which has already permitted us to perform experiments that would have been impossible to carry out with transient expression in *Xenopus* oocytes.

Another advantage of this stable expression system is that we can now begin to study aspects of the cell biology of the AChR that have been impossible to address in electrocytes or *Xenopus* oocytes, such as assembly, modulation, and nerve-induced clustering. The temperature sensitive effect on assembly, in particular, may prove valuable in studies of the assembly process. Certain structural studies might also be best performed with our expression system. For example, having large quantities of AChR's expressed on the surface of cultured cells will allow easy access to surface subunit epitopes by monoclonal antibodies directed against different structural and functional domains (35). This line of experimentation may help to define the topology of folding of the individual subunits in the plane of the membrane (6, 36) and thus provide more insight into predicting the folding patterns of transmembrane domains of proteins from hydropathy profiles (37). Such information will not only be of use in determining the AChR subunit topology, but it is likely to also be applicable to studies of other closely related proteins such as the ligand-gated glycine (38) and γ -aminobutyric acid (39) (GABA) receptor-channels.

REFERENCES AND NOTES

1. D. M. Fambrough, *Physiol. Rev.* **59**, 165 (1979); A. Karlin, *The Cell Surface and Neuronal Function*, C. W. Cotman, G. Poste, G. L. Nicolson, Eds. (North-Holland, Amsterdam, 1980), vol. 6, p. 191; B. M. Conti-Tronconi and M. A. Raftery, *Annu. Rev. Biochem.* **51**, 491 (1982); J.-L. Popot and J.-P. Changeux, *Physiol. Rev.* **64**, 1162 (1984); J. O. Dolly and E. A. Barnard, *Biochem. Pharmacol.* **33**, 841 (1984); R. Anholt, J. Lindstrom, M. Montal, *The Enzymes of Biological Membranes*, A. Martonosi, Ed. (Plenum, New York, 1984), vol. 3, p. 335; M. P. McCarthy, J. P. Earnest, E. F. Young, S. Choe, R. M. Stroud, *Annu. Rev. Neurosci.* **9**, 383 (1986); T. Claudio, *Trends Pharmacol. Sci.* **7**, 308 (1986); A. Maclicke, in *Handbook of Experimental Pharmacol.*, V. P. Whittaker, Ed. (Springer-Verlag, New York, in press), the volume title is *The Cholinergic Synapse*.
2. M. Mishina et al., *Nature (London)* **313**, 364 (1985).
3. M. M. White, K. Mixer-Mayne, H. A. Lester, N. Davidson, *Proc. Natl. Acad. Sci. U.S.A.* **82**, 4852 (1985).
4. T. Claudio, *ibid.* **84**, 5967 (1987).
5. R. Kucherlapati, Ed., *Gene Transfer* (Plenum Press, New York, 1986).
6. T. Claudio, M. Ballivet, J. Patrick, S. Heinemann, *Proc. Natl. Acad. Sci. U.S.A.* **80**, 1111 (1983).
7. D. M. Robins, R. Axel, A. S. Henderson, *J. Mol. Appl. Genet.* **1**, 191 (1981).
8. F. L. Graham and A. J. van der Eb, *Virology* **52**, 456 (1973).
9. M. Wigler et al., *Proc. Natl. Acad. Sci. U.S.A.* **76**, 1373 (1979).
10. T. Maniatis, E. F. Fritsch, J. Sambrook, Eds., *Molecular Cloning: A Laboratory Manual* (Cold Spring Harbor Laboratory, Cold Spring Harbor, NY, 1982).
11. E. Southern, *J. Mol. Biol.* **98**, 503 (1975).
12. T. Claudio, H. L. Paulson, D. Hartman, S. Fine, F. J. Sigworth, *Curr. Top. Membr. Transp.* **29**, in press.
13. N. J. Proudfoot and G. G. Brownlee, *Nature (London)* **263**, 211 (1976).
14. T. Claudio, unpublished observation.
15. C. M. Gorman, B. H. Howard, R. Reeves, *Nucleic Acids Res.* **11**, 7632 (1983).
16. T. Claudio and M. A. Raftery, *Arch. Biochem. Biophys.* **181**, 484 (1977).
17. S. Numa et al., *Cold Spring Harbor Symp. Quant. Biol.* **48**, 57 (1983).
18. R. Kornfeld and S. Kornfeld, *Annu. Rev. Biochem.* **54**, 631 (1985).
19. N. Fujita et al., *Science* **231**, 1284 (1986).
20. S. Sine and P. Taylor, *J. Biol. Chem.* **254**, 3315 (1979).
21. M. Weber and J.-P. Changeux, *Mol. Pharmacol.* **10**, 1 (1974).
22. C. Hyman and S. C. Froehner, *J. Cell. Biol.* **96**, 1316 (1983).
23. G. Weiland, B. Georgia, V. T. Wee, C. R. Chignell, P. Taylor, *Mol. Pharmacol.* **12**, 1091 (1976).
24. W. E. Brown and A. V. Hill, *Proc. R. Soc. London B* **94**, 297 (1922).
25. S. Sine and P. Taylor, *J. Biol. Chem.* **256**, 6692 (1981).
26. R. R. Neubig and J. B. Cohen, *Biochemistry* **18**, 5464 (1979).
27. G. Weiland and P. Taylor, *Mol. Pharmacol.* **15**, 197 (1979).
28. D. Blangy, H. Buc, J. Monod, *J. Mol. Biol.* **29**, 13 (1967).
29. S. Sine, unpublished observation.
30. O. P. Hamill, A. Marty, E. Neher, B. Sakmann, F. J. Sigworth, *Pfluegers Arch. Gesamte Physiol. Menschen Tiere* **391**, 85 (1981).
31. J. W. Walker, K. Takeyasu, M. G. McNamee, *Biochemistry* **21**, 5384 (1982); G. P. Hess, E. B. Pasquale, J. W. Walker, M. G. McNamee, *Proc. Natl. Acad. Sci. U.S.A.* **79**, 963 (1982).
32. K. Imoto et al., *Nature (London)* **324**, 670 (1986).
33. P. Labarca, J. Lindstrom, M. Montal, *J. Gen. Physiol.* **83**, 473 (1984).
34. D. W. Tank, R. L. Huganir, P. Greengard, W. W. Webb, *Proc. Natl. Acad. Sci. U.S.A.* **80**, 5129 (1983).
35. W. J. LaRochelle, B. E. Wray, R. Sealock, S. C. Froehner, *J. Cell. Biol.* **100**, 684 (1985).
36. R. H. Guy, *Biophys. J.* **45**, 249 (1984); J. Finer-Moore and R. M. Stroud, *Proc.*

- Natl. Acad. Sci. U.S.A.* **81**, 155 (1984); M. Ratnam, D. L. Nguyen, J. Rivier, P. B. Sargent, J. Lindstrom, *Biochemistry* **25**, 2633 (1986).
37. T. P. Hopp and K. R. Woods, *Proc. Natl. Acad. Sci. U.S.A.* **78**, 3824 (1981); J. Kyte and R. F. Doolittle, *J. Mol. Biol.* **157**, 105 (1982); D. M. Engelman, T. A. Steitz, A. Goldman, *Annu. Rev. Biophys. Biophys. Chem.* **15**, 321 (1986).
38. G. Grenningloh *et al.*, *Nature (London)* **328**, 215 (1987).
39. P. R. Schofield *et al.*, *ibid.* **328**, 221 (1987).
40. S. Subramani, R. C. Mulligan, P. Berg, *Mol. Cell. Biol.* **1**, 854 (1981).
41. A. Pellicer, M. Wigler, R. Axel, S. Silverstein, *Cell* **14**, 133 (1978).
42. A. P. Feinberg and B. Vogelstein, *Biochemistry* **132**, 6 (1983).
43. J. M. Chirgwin, A. E. Przybyla, R. J. MacDonald, W. J. Rutter, *ibid.* **18**, 5294 (1979).
44. J. Bernhardt and E. Neumann, *Proc. Natl. Acad. Sci. U.S.A.* **75**, 3756 (1978).
45. F. J. Sigworth and S. M. Sine, *Biophys. J.*, in press, 1987.
46. Supported by NIH grants NS 21714 (T.C.) and NS 21501 (F.J.S.) and postdoctoral fellowship award from the American Heart Association 11-108-878 (W.N.G.) and NIH award NS 07102 (A.S.).

28 September 1987; accepted 17 November 1987



"With all I've learned about psychology recently, establishing who's naughty and who's nice is not as simple as it used to be."